Journal of Alloys and Compounds 815 (2020) 152280

Contents lists available at ScienceDirect

Journal of Alloys and Compounds

journal homepage: http://www.elsevier.com/locate/jalcom

Hierarchical porous carbons derived from leftover rice for high performance supercapacitors

Zhimin Zou, Chunhai Jiang*

Fujian Provincial Key Laboratory of Functional Materials and Applications, Institute of Advanced Energy Materials, School of Materials Science and Engineering, Xiamen University of Technology, 600 Ligong Road, Jimei District, Xiamen, 361024, China

ARTICLE INFO

Article history:
Received 13 July 2019
Received in revised form
11 September 2019
Accepted 13 September 2019
Available online 14 September 2019

Keywords:
Supercapacitors
Porous carbons
Electrode
Leftover rice
Biomass

ABSTRACT

Biomass-derived porous carbons have been extensively investigated as potential electrode materials of electrochemical energy storage devices. Herein, hierarchical porous carbons with high specific surface area and large mesoporosity are successfully prepared from leftover rice, a common meal surplus, benefiting from its unique swelled structure and the activation effect of potassium hydroxide. The hierarchical porous carbons exhibit outstanding electrochemical energy storage performances in 1 M $TEABF_4$/PC (propylene carbonate) electrolyte, including a high specific capacitance of 153.2 F g^{-1} at 0.2 A g^{-1} based on the active material, a high specific energy density of 22.6 Wh kg^{-1} at a power density of 21,503 W kg^{-1} based on the cells and over 87% capacitance retentions after 10,000 cycles at 1 A g^{-1}. Such excellent electrochemical performances demonstrate that leftover rice can be potentially applied as bioresource for high property porous carbon electrode materials of supercapacitors.

1. Introduction

Electrochemical energy storage devices, including rechargeable batteries and supercapacitors, are the major power sources of portable electronic devices and electric vehicles in nowadays. Comparing to rechargeable batteries such as Li-ion batteries and lead-acid batteries, supercapacitors are advantageous in terms of excellent high power density and ultralong cycle life [1–4]. However, as far as energy density is concerned, applications of supercapacitors are restricted. According to the formula of specific energy density, $E = 0.5CV^2$ (where C and V represent the specific cell capacitance and working voltage of the supercapacitors, respectively), increasing the voltage window and specific capacitance of electrode materials are the two major strategies to improve the energy density of supercapacitors [5]. Concerning to the former strategy, exploring novel electrolytes with wider voltage window or higher stability has been frequently investigated [6,7]. As for the latter, exploration of novel electrode materials with high specific capacitance has been the dominant research topic in recent years [8].

The dominant electrode materials for commercially available supercapacitors are still activated carbons produced majorly from coconut shells [9]. However, the quality of activated carbons depends greatly on the selected coconut shells. In addition, because of the dedicated activation procedure required for controlling the specific surface area, pore volume and pore size distribution desired for high performance supercapacitors, high quality activated carbons are still too expensive for scale applications. Under this circumstance, producing high quality yet low cost activated carbons has been the ongoing research interest of many groups [10]. Thanks to the fruitful natural structures, agricultural wastes such as rice husk [11,12], peanut shell [13], corncob [14], and bagasse [15], etc., have been successfully employed as alternative biomass resources for preparation of porous carbons with diverse texture properties. Another family of abundant raw materials, the so-called meal surplus, have also been used for porous carbon preparation. For examples, crab shells [16], shrimp shells [17] and animal bones [18] have been proven of good resources for hierarchical porous carbons. However, as one popular meal surplus, leftover rice has not yet been used as carbon resource. It is known that rice contains about 75 wt% starch and cellulose, 7–8 wt% protein, and 1.3–1.8 wt% aliphatics, which can all be converted to carbon by pyrolysis. In addition, similar to popcorn [19], the cooked rice possesses a swelled structure, which is beneficial for fabrication of hierarchical porous carbons. Herein, leftover rice was used to prepare porous carbons for potential electrode materials of supercapacitors by integrating freeze drying and KOH activation

* Corresponding author.
E-mail address: chjiang@xmut.edu.cn (C. Jiang).

https://doi.org/10.1016/j.jallcom.2019.152280
0925-8388/

processes. It will be shown that benefiting from the unique swelled structure and activation effect of KOH, hierarchical porous carbons (HPCs) with high specific surface area (over 2000 $m^2 g^{-1}$) and large pore volume (>1.8 $cm^3 g^{-1}$) could be facilely prepared. The electrochemical tests in organic electrolyte indicated that the porous carbon electrodes could deliver a high specific capacitance of 153.2 F g^{-1} at 0.2 A g^{-1}, and a high energy density of 22.6 Wh kg^{-1} even at a power density of 21,503 W kg^{-1} (based on the active mass of both electrodes). The detailed preparation, characterizations and electrochemical performances of the hierarchical porous carbons derived from leftover rice are reported.

2. Experimental details

2.1. Preparation and characterizations of HPCs

Hierarchical porous carbons were prepared from the leftover rice collected from the dining hall of Xiamen University of Technology. The preparation process included freeze drying, pre-carbonization and KOH chemical activation steps in sequence, as shown in Scheme 1. In detail, the leftover rice was frozen-dried at -50 °C for more than 20 h and pre-carbonized in air at 300 °C for 2 h. After manual grinding, the precursors were mixed with KOH in the mass ratios of 1–3 in an appropriate amount of water. The activations were carried out at 850 °C for 4 h in a tube furnace protected by flowing nitrogen. After washing by diluted HCl solution (1 M) and de-ionized water and drying at 80 °C for 12 h, HPCs were obtained. According to the mass ratio of KOH used, the porous carbons were marked as HPCs-1, HPCs-2 and HPCs-3, respectively.

The phase and microstructures of the obtained HPCs were characterized by X-ray diffraction (XRD, Rigaku MiniFlex600), scanning electron microscope (SEM, Zeiss Sigma 500), and transmission electronic microscope (TEM, FEI Talos F200s), respectively. The texture properties of the porous carbons including specific surface area (Brunauer–Emmert–Teller, BET), total pore volume (V_t), micropore volume (V_{mic}), and pore size distributions were analyzed based on the N_2 adsorption/desorption isotherms measured by a porosimetry analyzer (Micromeritics, ASAP 2020 Plus) at 77 K.

2.2. Electrochemical characterizations

The energy storage performances of the prepared HPCs were evaluated by means of symmetric electrical double layer capacitors (EDLCs) in 1 M $TEABF_4$ dissolved in propylene carbonate (PC). The detailed electrode preparation and electrochemical tests were similar to that of our previous publications [20,21]. The active mass in each electrode was about 1.5–1.8 mg cm^{-2}.

3. Results and discussion

Rice is an assembly of hydrocarbons, such as starch, protein, and aliphatics, etc. It is the staple food of more than half the world's population. Also because of its popular, the amount of leftover rice produced every day is enormous, which is usually discarded as valueless garbage. In fact, benefiting from the high carbon content and swelled structure of the cooked rice, hierarchical porous carbons can be fabricated by integration of freeze-drying, pre-carbonization and KOH chemical activation treatments, as illustrated in Scheme 1.

The microstructures of the obtained HPCs were examined by SEM at first, as shown in Fig. 1a and b for HPCs-1, Fig. 1c and d for HPCs-2, Fig. 1e and f for HPCs-3, respectively. As seen from Fig. 1a, at a KOH mass ratio of 1:1, the carbon sample appears as irregular granulates of about ten to several tenths of micrometers in size. Seeing more closely to the surface of the carbon granulates, a highly porous structure can be clearly observed (Fig. 1b), although the carbon granulates shown in Fig. 1a look quite dense. When the KOH mass ratio was increased to 2:1, some of the carbon granulates were converted to foam-like structures (see Fig. 1c and d). Further increasing the KOH mass ratio to 3:1, almost all the carbon granulates became foam-like (Fig. 1e). Three-dimensional interconnected carbon foams with sheet-like thin struts and open pores of a few hundreds of nanometers in diameters were clearly observed (Fig. 1f). This meant that the amount of KOH activating reagent was very crucial to the foam structure of the carbon samples. A higher mass ratio of KOH had resulted in more severe etching of the carbon matrix, leading to sufficient pore widening, and finally hierarchical porous structure. The effect of freeze drying on the porous structure of the leftover rice-derived carbon samples was also investigated. Fig. S1 in the supplementary document shows the SEM images of the carbon samples directly pyrolized from the frozen-dried (a and b) and conventionally dried (c and d) leftover rice. As can be seen, the freeze-drying treatment preserved the swelled structure of the cooked rice. Instead, conventional drying resulted in less porous structure in the pyrolized carbon. In both cases, the samples show dense carbon matrix at high resolution, which inversely proved that the highly porous structure of the HPCs were introduced by KOH activation.

To further explore the microstructural evolutions of the porous carbons associated with the variations of KOH mass ratios, TEM

Scheme 1. Schematic illustration of the preparation process of the hierarchical porous carbons from leftover rice.

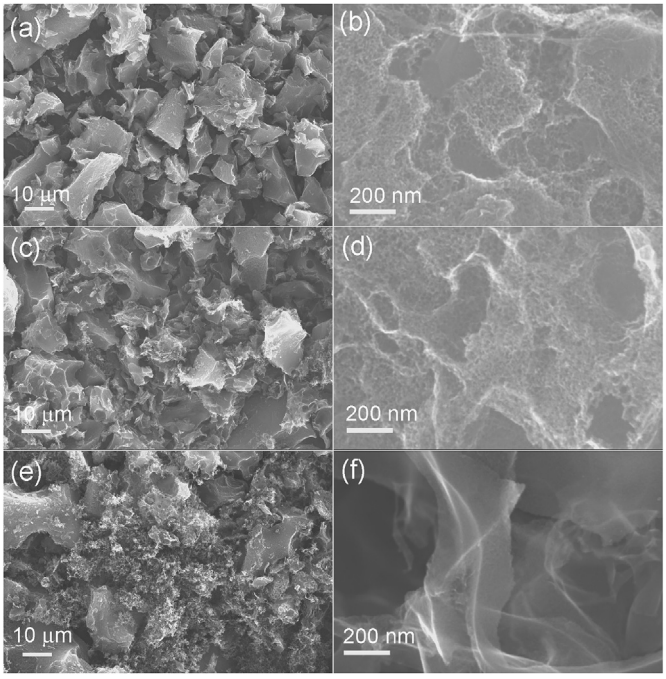

Fig. 1. SEM images of the leftover rice-derived HPCs-1 (a and b), HPCs-2 (c and d), and HPCs-3 (e and f).

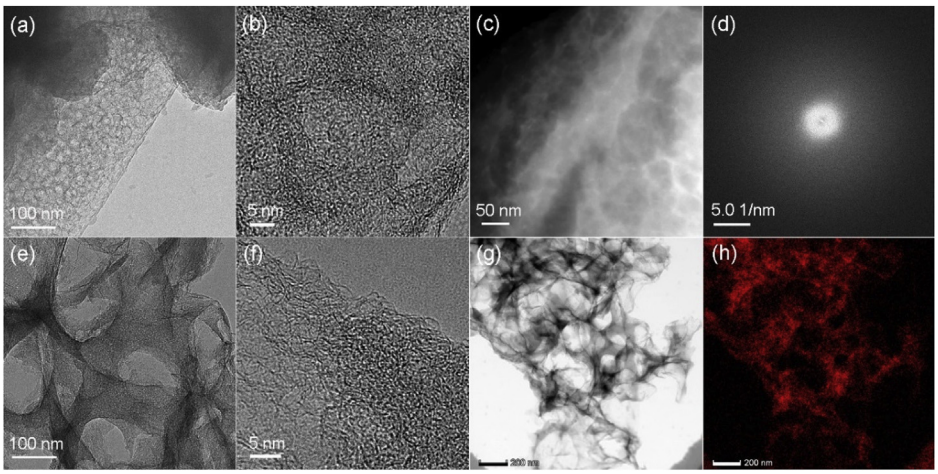

Fig. 2. TEM characterization of the leftover rice-derived HPCs-1 (a–d) and HPCs-3 (e–h).

observations in both bright field and HADDF modes were carried out. Fig. 2 shows the typical bright field TEM image (a), high resolution TEM (HRTEM) image (b), HADDF image (c), and the selected area diffraction pattern of HPCs-1. As can be seen in Fig. 2a, the HPCs-1 sample exhibits sheet-like structure consisting of a large amount of nanosized pores. The HRTEM image (Fig. 2b) further confirms that the pore sizes are in the level of several tens of nanometers, which are connected by amorphous carbon walls of a few nanometers in thickness. Such a porous structure within the carbon matrix can be clearly seen from the HADDF image shown in Fig. 2c. The amorphous nature of the carbon sample is further identified by the selected area diffraction pattern (Fig. 2d). The microstructures characterized by TEM observation are well consistent to that of SEM images shown in Fig. 1a and b. That is, although the carbon granulates look dense, the carbon matrix is rich of mesopores and micropores. When the KOH mass ratio was increased to 3, the microstructural morphology of the porous carbon changed a lot, as shown in Fig. 2e–h. A bright field TEM image shown in Fig. 2e evidently confirmed the foam-like structure as observed in Fig. 1e and f. Unlike the small pores in HPCs-1, the pore sizes in HPCs-3 were much larger, attributing to the much severe etching effect of KOH. As seen in Fig. 2f, the pore walls were also composed of disordered amorphous structure, typical for porous carbons obtained by KOH activation. The HADDF image shown in Fig. 2g once again illustrated the hierarchical porous structure of HPCs-3. The pores of about 100–200 nm in diameters were three-dimensionally interconnected, forming highly porous carbon foam. The element map in Fig. 2h demonstrates that the sample is almost completely composed of carbon, although trace amounts of nitrogen and calcium are present in the original leftover rice.

Nitrogen adsorption/desorption isotherms were measured at 77 K on the HPCs to analyze the texture properties, as displayed in Fig. 3a. The pore size distributions calculated using the quenched solid state functional theory (QSDFT) are shown in Fig. 3b. The corresponding texture properties are compared in Table 1. As can be seen in Fig. 3a, the isotherms of all the carbon samples can be treated as a mixture of the type I and type IV isotherms according to the IUPAC classification [22]. The sharp increase of N_2 adsorption at the low relative pressure indicates the presence of micropores. The continuous increase of the N_2 adsorption along with the increase of P/P_0, and the obvious hysteresis loops between the adsorption and desorption branches, reveal the existence of high volumetric mesopores. The specific surface areas (BET) of HPCs-1, HPCs-2 and HPCs-3 are 1,922, 2,166, and 2,184 $m^2 g^{-1}$, with the corresponding total pore volumes of 1.497, 1.730, and 1.839 $cm^3 g^{-1}$, respectively (see Table 1). As determined by *t*-pot method, the ratios of micropore volumes in the HPCs-1, HPCs-2 and HPCs-3 samples are 28.56%, 22.9% and 19.4%, respectively. HPCs-2 and HPCs-3 show higher ratios of mesopores in the total pore volume than that of HPCs-1. Also, the mean pore diameters of HPCs-2 and HPCs-3 are 3.19 and 3.36 nm, respectively, higher than that of HPCs-1, 3.11 nm. This suggests that more adequate etching of the leftover rice-derived carbon matrix has occurred at a higher KOH mass ratio. The pore size distributions were determined from the N_2 adsorption/desorption isotherms using the QSDFT equilibrium model based on slit pores. As shown in Fig. 3b, HPCs-2 and HPCs-3 possess higher volumetric portion of mesopores than HPCs-1. By contrast, the portions of micropores in HPCs-1 is slightly higher. Such a highly mesoporous structure can be expected to provide sufficient channels for the diffusion of electrolyte ions, which may in turn improve the power density of supercapacitors.

The XRD patterns and Raman spectra of the HPCs are shown in Fig. 3c and d, respectively. Both characterizations indicate the amorphous nature of the carbon samples. In XRD patterns, the (0 0 2) peak at about $2\theta = 26^\circ$ is very weak in all samples, suggesting their low degree of graphitization (Fig. 3c). There are two typical peaks at 1,340 cm^{-1} and 1,590 cm^{-1} in Raman spectra, which are correlated to the defects and disorder (D band), and the graphitic structure (G band) in the porous carbons, respectively [23]. The intensity ratios of D band to G band (I_D/I_G, I_D and I_G are the integrated areas of D and G peaks) indicate the degree of disorder, which are 2.19, 2.68, and 2.95 for HPCs-1, HPCs-2, and HPCs-3, respectively. This means that increasing the KOH mass ratio has resulted in more amorphous structure of the leftover rice-derived porous carbons, attributing to the more severe etching effect.

The surface chemical properties of the hierarchical porous carbons were characterized by XPS. Fig. 3e and f show the survey scan and C1s core scan of the relevant XPS spectra, respectively. As seen from Fig. 3e, except the O1s and C1s peaks, no other evident peaks are detected, indicating that the materials are majorly composed of carbon element, together with some oxygen-containing surface functional groups. The C1s peak can be deconvoluted into three peaks localized at 284.6, 286.2, and 289.2 eV, respectively, which are normally ascribed to the sp^2 C=C, C=O, and O–C=O bonding [23,24]. This again confirms that the porous carbons are mainly composed of carbon element, but with some oxygen-rich functional groups.

The electrochemical performances of HPCs were evaluated by

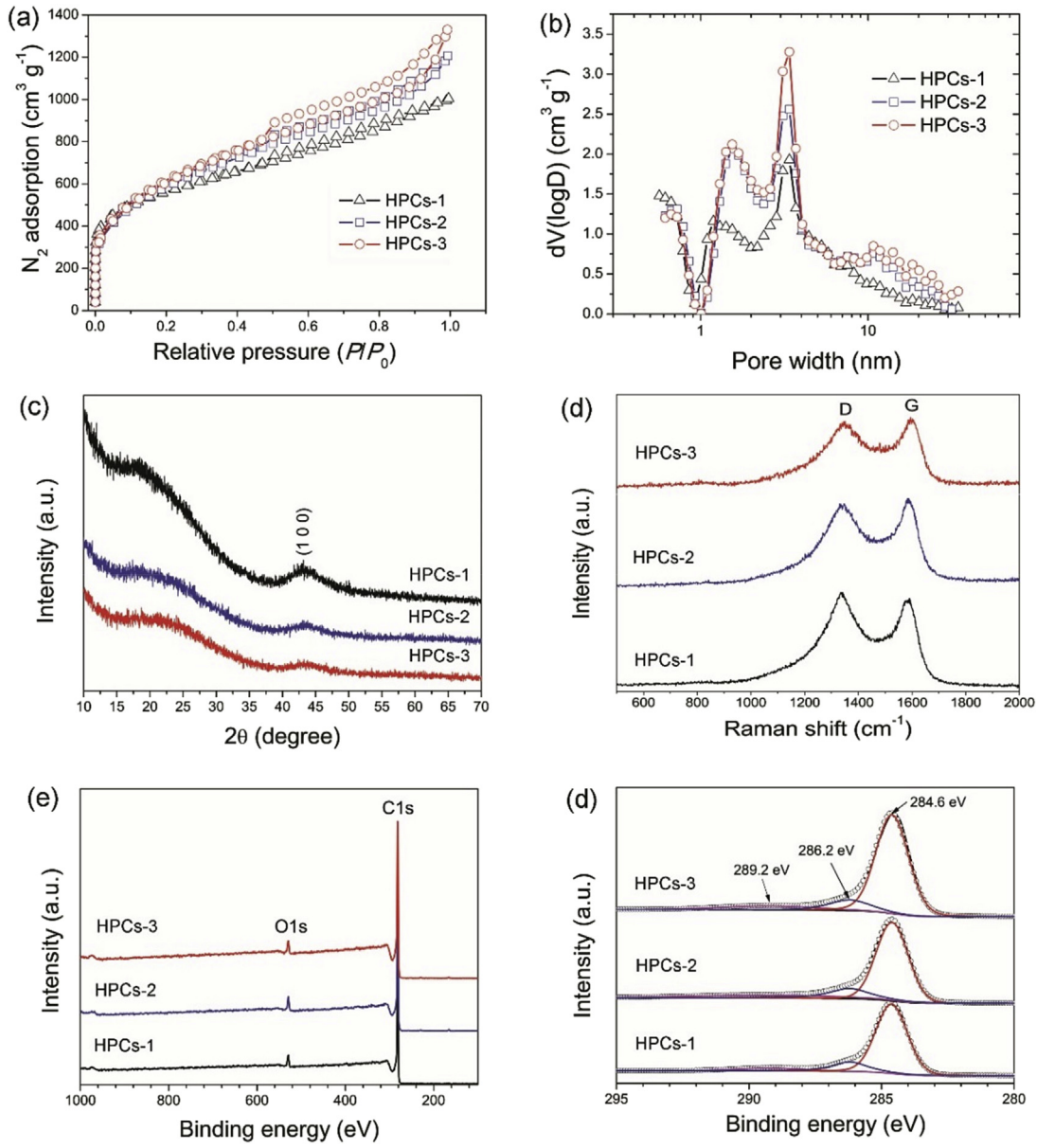

Fig. 3. N_2 adsorption/desorption isotherms (a), pore size distributions (b), XRD patterns (c), Raman spectra (d), XPS survey scan (e) and C1s core scan (f) of the HPCs.

Table 1
Texture properties of the leftover rice-derived HPCs.

Sample	S_{BET} ($m^2\ g^{-1}$)	S_{mic} ($m^2\ g^{-1}$)	V_t ($cm^3\ g^{-1}$)	V_{mic} ($cm^3\ g^{-1}$)	V_{mic}/V_t	D_{mean} (nm)
HPCs-1	1922	883	1.497	0.426	0.285	3.11
HPCs-2	2166	863	1.730	0.396	0.229	3.19
HPCs-3	2184	731	1.839	0.356	0.194	3.36

symmetric electrical double layer capacitors (EDLCs) using 1 M $TEABF_4$/PC as the electrolyte. At first, cyclic voltammetry (CV) measurements were performed at various scan rates ranging from 10 to 300 mV s^{-1}. Fig. 4a and b show the CV curves of the cells measured at 10 and 300 mV s^{-1}, respectively. All the cells show quite good rectangular CV curves at both 10 and 300 mV s^{-1}, demonstrating their excellent capacitive energy storage behavior. As shown in both Fig. 4a and b, the specific capacitances of the HPCs as estimated from the areas of CV curves increase with their specific surface areas. Moreover, cells HPCs-2 and HPCs-3 show better preserved rectangular CV curves than cell HPCs-1 at 300 mV s^{-1}, suggesting that the larger mesopore volumes in these samples have played an important role on the fast charge storage. The galvanostatic charge and discharge (GCD) curves of the three cells measured at constant current densities of 0.2 and 5 A g^{-1} are shown in Fig. 4c and d, respectively. The GCD curves of the cells at other current densities can be found in the supplementary document. All the cells show well-preserved triangle shape GCD curves at 0.2 A g^{-1}, again illustrating their good electrical double layer charge storage behavior. The specific discharge capacitances of cells HPCs-

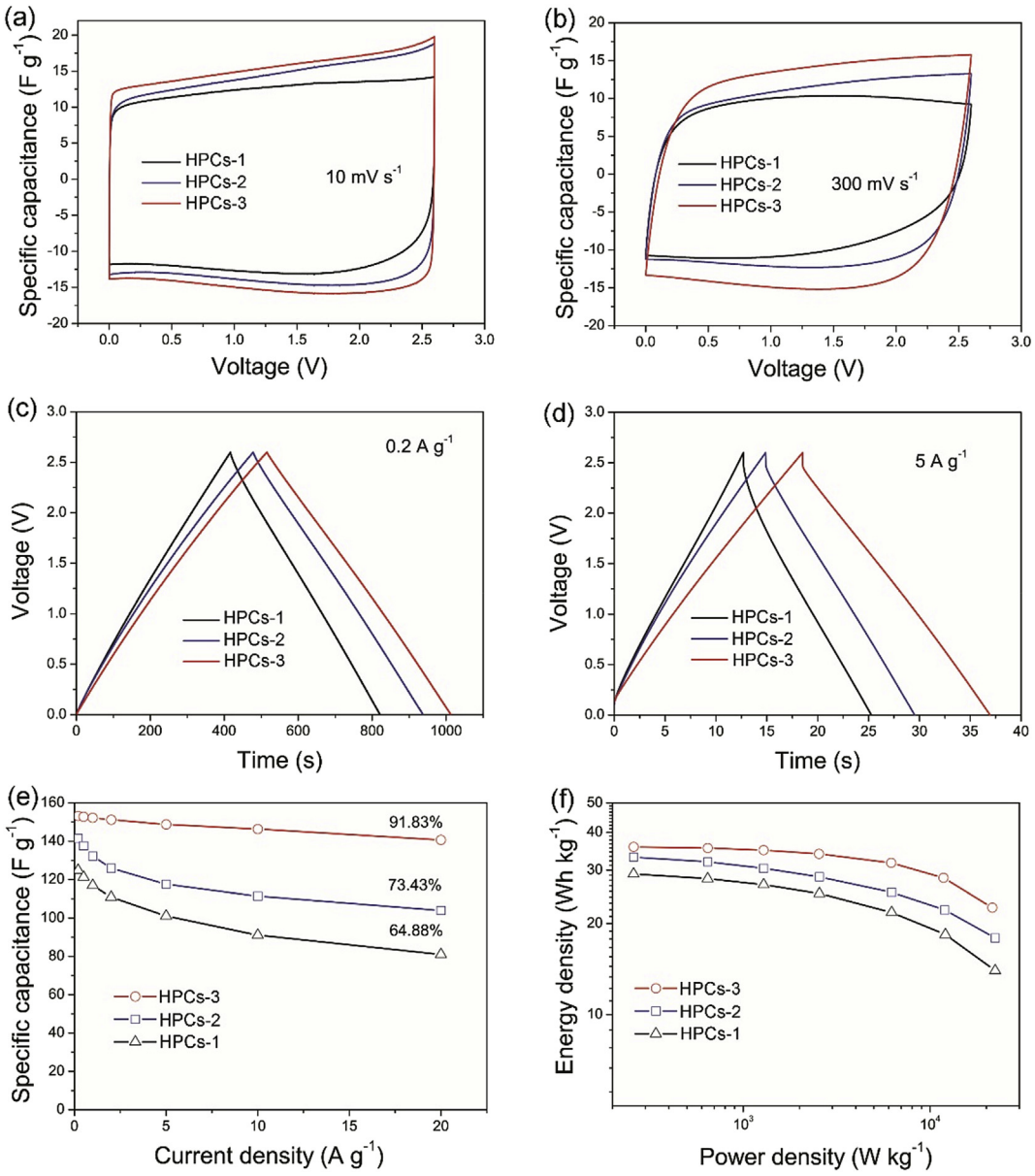

Fig. 4. Electrochemical properties of the supercapacitors assembled from HPCs-1, HPCs-2 and HPCs-3 electrodes, CV curves measured at scan rates of (a) 10 mV s^{-1} and (b) 300 mV s^{-1}, GCD curves tested at 0.2 A g^{-1} (c) and 5 A g^{-1} (d), rate performance (e), and ragone plots (f).

1, HPCs-2 and HPCs-3 at this current density are 31.2, 35.4 and 38.3 F g^{-1}, respectively. When the current density increases to 5 A g^{-1}, the GCD curves remain good triangle shape, but with diverse capacity retentions. The specific discharge capacitances of the corresponding cells become 25.3, 29.4, and 37.2 F g^{-1}, being about 81%, 83%, and 97% of those measured at 0.2 A g^{-1}, respectively. This clearly indicates that the supercapacitors assembled from the hierarchical porous carbons possess excellent energy storage performance at high power densities. As further identified in Fig. 4e, the specific capacitances of HPCs-1, HPCs-2 and HPCs-3 at 0.2 A g^{-1} are 124.8, 141.5 and 153.2 F g^{-1}, whereas the corresponding values at 20 A g^{-1} drop to 64.88%, 73.43% and 91.83% of those at 0.2 A g^{-1}, respectively. That means that cell HPCs-3 owns obvious better rate capability than the other two samples. The rapid capacitance degradation of HPCs-1 and HPCs-2 can be correlated to their smaller pore sizes, which may restrict the motion of large organic electrolyte ions [25]. By contrast, the hierarchical porous structure of HPCs-3 together with the thin pore walls can expose more accessible surface to the electrolyte, leading to higher capacitance even at short charge-discharge time. The excellent energy storage properties of the hierarchical porous carbons are further demonstrated by the ragone plots, as shown in Fig. 4f. At a low power density of about 259 W kg^{-1}, cells HPCs-1, HPCs-2 and HPCs-3 show energy densities of about 29.2, 33.2 and 35.8 Wh kg^{-1}, respectively. At a high power density of 21,503 W kg^{-1}, cell HPCs-3 still exhibits an energy density of 22.6 Wh kg^{-1}, much higher than those of cells HPCs-1 (14 Wh kg^{-1} at 22,299 W kg^{-1}) and HPCs-2 (17.9 Wh kg^{-1} at 22,296 W kg^{-1}). The energy storage performance of cell HPCs-3 is among the best data achieved on biomass-derived porous carbon electrodes in similar electrolyte, as listed in Table 2. This indicates that the leftover rice-derived hierarchical porous carbons can be promising electrode materials for high energy and high power supercapacitors.

The cycle performances of the supercapacitors were tested at

Table 2
Comparison of biomass-derived carbon electrode materials for supercapacitors in organic electrolyte.

Carbon samples	Electrolyte	Power density (kW kg^{-1})	Energy density (Wh kg^{-1})	Ref.
Silkworm cocoon	1 M $TEABF_4$/AN	3.12	34.4	[26]
Pomelo peels	1 M $TEABF_4$/PC	21.5	25.3	[27]
Peanut shell	1 M $Et4NBF_4$/PC	1.0	19.3	[28]
Hemp stem	1.8 M $TEABF_4$/PC	21	19.8	[29]
Leonardite fulvic acid	1 M $TEABF_4$/PC	5.89	23.3	[30]
Paper pulp	1 M $TEABF_4$/AN	20	5.45	[31]
Cinnamon sticks	1 M $NaClO_4$/(EC + DMEC)	6	28	[32]
Kapok fibers	1 M $TEABF_4$/PC	24	24	[20]
Leftover rice	1 M $TEABF_4$/PC	21.5	22.6	This work

1 A g^{-1} for 10,000 cycles, as shown in Fig. 5a. The capacity retentions of cells HPCs-1, HPCs-2 and HPCs-3 after 10,000 cycles were about 88.7%, 87.2% and 87.6%, respectively, demonstrating quite good cycle stability. This stable cycle performance can be correlated to the hierarchical structure of the leftover rice-derived porous carbon electrode materials, which might have facilitated the ion transport. The electrochemical impedance spectra of the test cells were measured after the cycling tests, see Fig. 5b. The Nyquist plots show a straight line in low-frequency range and a half circle in high-frequency range. The straight line in the low-frequency range represents the ion diffusion resistance in the bulk electrode. In general, the slop of the straight line is proportional to the diffusion rate. From Fig. 5b one can easily distinguish that the ion diffusions in electrodes HPCs-2 and HPCs-3 are much faster than that in HPCS-1, which is in good agreement with their better capacitive behavior. The equivalent series resistances (R_s) can be obtained from the intersections of the half circles in the high-frequency range on X-axis. The diameters of the half circles represent the transport resistances (R_{ct}) across the electrode/electrolyte interface. As fitted by the ZView software, the equivalent series resistances of cells HPCs-1, HPCs-2 and HPCs-3 are 1.69, 1.36 and 1.60 Ω, while the corresponding charge transfer resistances are 3.39, 3.31 and 2.93 Ω, respectively. This demonstrates that the charge transfer within the more porous electrodes has been improved. These electrochemical performances strongly suggest that the hierarchical porous carbons derived from leftover rice can be ideal electrode materials of high power supercapacitors.

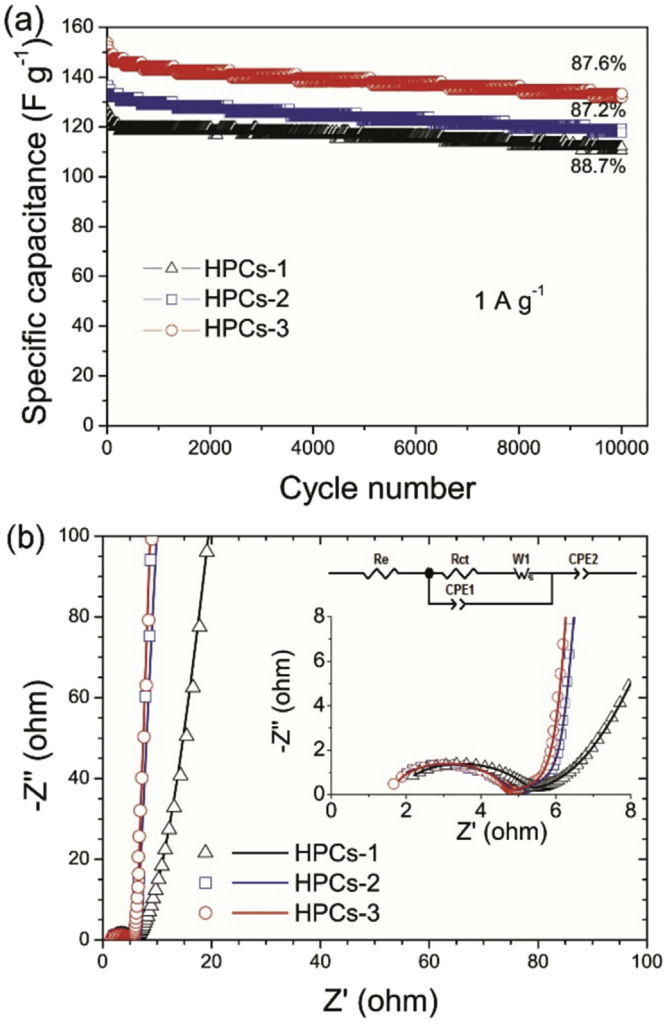

Fig. 5. The cycle performances of cells HPCs-1, HPCs-2 and HPCs-3 tested at 1 A g^{-1} (a), and the Nyquist plots for the electrochemical impedance spectra measurements (b). The Fig. 5b insets are the expanded EIS spectra and the equivalent circuit.

4. Conclusions

In this work, a common meal surplus, leftover rice, was used as raw material for hierarchical porous carbon electrode materials of supercapacitors. Thanks to the unique swelled structure of the cooked rice and the activation effect of KOH, hierarchical porous carbons with high specific surface area over 2000 $m^2 g^{-1}$ and large pore volume larger than 1.8 $cm^3 g^{-1}$ were prepared. When tested as electrode materials of supercapacitors in 1 M $TEABF_4$/PC electrolyte, the hierarchical porous carbons electrode exhibited high specific capacitance (153.2 F g^{-1} at 0.2 A g^{-1}), excellent high power energy storage performance (22.6 Wh kg^{-1} at 21,503 W kg^{-1}) and stable cycle performance (over 87% capacitance retentions after 10,000 cycles at 1 A g^{-1}). These excellent electrochemical performances demonstrated that leftover rice can be potential bioresource for high property porous carbon electrode materials of supercapacitors.

Acknowledgements

The authors gratefully acknowledge the financial supports from the Natural Science Foundation projects (No. 2016J01746and 2018J01429) and Guidance Project (No. 2016H0038) of Fujian Province, the Guiding project of Xiamen Municipal Bureau of Science and Technology (No. 3502Z20179022), and the Program for Innovative Research Team in Science and Technology in Fujian Province University.

Appendix A. Supplementary data

Supplementary data to this article can be found online at https://doi.org/10.1016/j.jallcom.2019.152280.

References

[1] Y. Wang, Y. Song, Y. Xia, Electrochemical capacitors: mechanism, materials, systems, characterization and applications, Chem. Soc. Rev. 45 (2016) 5925–5950.

[2] G. Wang, L. Zhang, J. Zhang, A review of electrode materials for electrochemical supercapacitors, Chem. Soc. Rev. 41 (2012) 797–828.

[3] P. Simon, Y. Gogotsi, B. Dunn, Where do batteries end and supercapacitors begin? Science 343 (2014) 1210–1211.

[4] Z. Liu, G. Liang, Y. Zhan, H. Li, Z. Wang, L. Ma, Y. Wang, X. Niu, C. Zhi, A soft yet device-level dynamically super-tough supercapacitor enabled by an energy-dissipative dual-crosslinked hydrogel electrolyte, Nano Energy 58 (2019) 732–742.

[5] J. Yan, Q. Wang, T. Wei, Z. Fan, Recent advances in design and fabrication of electrochemical supercapacitors with high energy densities, Adv. Energy Mater. 4 (2014), 1300816.

[6] Y. Wang, F. Chen, Z. Liu, Z. Tang, Q. Yang, Y. Zhao, S. Du, Q. Chen, C. Zhi, A highly elastic and reversibly stretchable all-polymer supercapacitor, Angew. Chem. Int. Ed., 0, DOI: http://dx.doi.org/10.1002/anie.201908985.

[7] Z. Wang, H. Li, Z. Tang, Z. Liu, Z. Ruan, L. Ma, Q. Yang, D. Wang, C. Zhi, Hydrogel electrolytes for flexible aqueous energy storage devices, Adv. Funct. Mater. 28 (2018), 1804560.

[8] Y. Wang, Q. Yang, Y. Zhao, S. Du, C. Zhi, Recent advances in electrode fabrication for flexible energy-storage devices, Adv. Mater. Technol. 4 (2019), 1900083.

[9] J. Mi, X.-R. Wang, R.-J. Fan, W.-H. Qu, W.-C. Li, Coconut-shell-based porous carbons with a tunable micro/mesopore ratio for high-performance supercapacitors, Energy Fuel 26 (2012) 5321–5329.

[10] H. Jin, J. Li, Y. Yuan, J. Wang, J. Lu, S. Wang, Recent progress in biomass-derived electrode materials for high volumetric performance supercapacitors, Adv. Energy Mater. 8 (2018), 1801007.

[11] D. Liu, W. Zhang, H. Lin, Y. Li, H. Lu, Y. Wang, Hierarchical porous carbon based on the self-templating structure of rice husk for high-performance supercapacitors, RSC Adv. 5 (2015) 19294–19300.

[12] E.Y.L. Teo, L. Muniandy, E.-P. Ng, F. Adam, A.R. Mohamed, R. Jose, K.F. Chong, High surface area activated carbon from rice husk as a high performance supercapacitor electrode, Electrochim. Acta 192 (2016) 110–119.

[13] M.-b. Wu, R.-c. Li, X.-j. He, H.-b. Zhang, W.-b. Sui, M.-h. Tan, Microwave-assisted preparation of peanut shell-based activated carbons and their use in electrochemical capacitors, N. Carbon Mater. 30 (2015) 86–91.

[14] W.-H. Qu, Y.-Y. Xu, A.-H. Lu, X.-Q. Zhang, W.-C. Li, Converting biowaste corncob residue into high value added porous carbon for supercapacitor electrodes, Bioresour. Technol. 189 (2015) 285–291.

[15] K. Zou, Y. Deng, J. Chen, Y. Qian, Y. Yang, Y. Li, G. Chen, Hierarchically porous nitrogen-doped carbon derived from the activation of agriculture waste by potassium hydroxide and urea for high-performance supercapacitors, J. Power Sources 378 (2018) 579–588.

[16] M. Fu, W. Chen, X. Zhu, B. Yang, Q. Liu, Crab shell derived multi-hierarchical carbon materials as a typical recycling of waste for high performance supercapacitors, Carbon 141 (2019) 748–757.

[17] F. Gao, J. Qu, C. Geng, G. Shao, M. Wu, Self-templating synthesis of nitrogen-decorated hierarchical porous carbon from shrimp shell for supercapacitors, J. Mater. Chem. A 4 (2016) 7445–7452.

[18] W. Huang, H. Zhang, Y. Huang, W. Wang, S. Wei, Hierarchical porous carbon obtained from animal bone and evaluation in electric double-layer capacitors, Carbon 49 (2011) 838–843.

[19] J. Hou, K. Jiang, R. Wei, M. Tahir, X. Wu, M. Shen, X. Wang, C. Cao, Popcorn-derived porous carbon flakes with an ultrahigh specific surface area for superior performance supercapacitors, ACS Appl. Mater. Interfaces 9 (2017) 30626–30634.

[20] Z. Zou, T. Liu, C. Jiang, Highly mesoporous carbon flakes derived from a tubular biomass for high power electrochemical energy storage in organic electrolyte, Mater. Chem. Phys. 223 (2019) 16–23.

[21] Z. Zou, J. Zhao, J. Xue, R. Huang, C. Jiang, Highly porous carbon spheres prepared by boron-templating and reactive H_3PO_4 activation as electrode of supercapacitors, J. Electroanal. Chem. 799 (2017) 187–193.

[22] J. Rouquerol, D. Avnir, C.W. Fairbridge, D.H. Everett, J.M. Haynes, N. Pernicone, J.D.F. Ramsay, K.S.W. Sing, U. KK, Recommendations for the characterization of porous solids (Technical Report), Pure Appl. Chem. 66 (1994) 1739–1758.

[23] W. Tian, Q. Gao, Y. Tan, Y. Zhang, J. Xu, Z. Li, K. Yang, L. Zhu, Z. Liu, Three-dimensional functionalized graphenes with systematical control over the interconnected pores and surface functional groups for high energy performance supercapacitors, Carbon 85 (2015) 351–362.

[24] H. Wang, Z. Xu, A. Kohandehghan, Z. Li, K. Cui, X. Tan, T.J. Stephenson, C.K. King'ondu, C.M.B. Holt, B.C. Olsen, J.K. Tak, D. Harfield, A.O. Anyia, D. Mitlin, Interconnected carbon nanosheets derived from hemp for ultrafast supercapacitors with high energy, ACS Nano 7 (2013) 5131–5141.

[25] H.J. Keh, S.B. Chen, Diffusiophoresis and electrophoresis of colloidal cylinders, Langmuir 9 (1993) 1142–1149.

[26] J. Sun, J. Niu, M. Liu, J. Ji, M. Dou, F. Wang, Biomass-derived nitrogen-doped porous carbons with tailored hierarchical porosity and high specific surface area for high energy and power density supercapacitors, Appl. Surf. Sci. 427 (2018) 807–813.

[27] F. Sun, L. Wang, Y. Peng, J. Gao, X. Pi, Z. Qu, G. Zhao, Y. Qin, Converting biomass waste into microporous carbon with simultaneously high surface area and carbon purity as advanced electrochemical energy storage materials, Appl. Surf. Sci. 436 (2018) 486–494.

[28] X. He, P. Ling, J. Qiu, M. Yu, X. Zhang, C. Yu, M. Zheng, Efficient preparation of biomass-based mesoporous carbons for supercapacitors with both high energy density and high power density, J. Power Sources 240 (2013) 109–113.

[29] W. Sun, S.M. Lipka, C. Swartz, D. Williams, F. Yang, Hemp-derived activated carbons for supercapacitors, Carbon 103 (2016) 181–192.

[30] Y. Ma, Y. Guo, C. Zhou, C. Wang, Biomass-derived dendritic-like porous carbon aerogels for supercapacitors, Electrochim. Acta 210 (2016) 897–904.

[31] H. Wang, Z. Li, J.K. Tak, C.M.B. Holt, X. Tan, Z. Xu, B.S. Amirkhiz, D. Harfield, A. Anyia, T. Stephenson, D. Mitlin, Supercapacitors based on carbons with tuned porosity derived from paper pulp mill sludge biowaste, Carbon 57 (2013) 317–328.

[32] R. Thangavel, K. Kaliyappan, H.V. Ramasamy, X. Sun, Y.-S. Lee, Engineering the pores of biomass-derived carbon: insights for achieving ultrahigh stability at high power in high-energy supercapacitors, ChemSusChem 10 (2017) 2805–2815.